



Published in final edited form as:

Biopolymers. 2008 November ; 89(11): 1032–1044. doi:10.1002/bip.21056.

Conformational studies of the α -helical 28–43 fragment of the B3 domain of the immunoglobulin binding protein G from *Streptococcus*

Agnieszka Skwierawska^{1,2}, Sylwia Rodziewicz-Motowidło³, Stanisław Ołdziej^{1,2}, Adam Liwo^{2,3}, and Harold A. Scheraga²

¹Laboratory of Biopolymer Structure, Intercollegiate Faculty of Biotechnology, University of Gdansk, Medical University of Gdańsk, Kładki 24, 80-922 Gdańsk, Poland ²Baker Laboratory of Chemistry and Chemical Biology, Cornell University, Ithaca, NY 14853-1301, USA ³Faculty of Chemistry, University of Gdańsk, ul. Sobieskiego 18, 80-952 Gdańsk, Poland

Abstract

To determine whether the α -helix in the B3 immunoglobulin binding domain of protein G from group G *Streptococcus* has conformational stability as an isolated fragment, we carried out a CD and NMR study of the 16-residue peptide in solution corresponding to this α -helix. Based on 2D H-NMR spectra recorded at three different temperatures (283, 305, and 313 K), it was found that this peptide is mostly unstructured in water at these temperatures. Weak signals corresponding to $i, i+3$ or $i, i+4$ interactions, which are characteristic of formation of turn-like structures, were observed in the ROE spectra at all temperatures. The absence of a stable three-dimensional structure of the investigated peptide supports an earlier study [Blanco, F. J.; Serrano, L. *Eur J Biochem* 1995, 230, 634–649] of a possible mechanism for folding of other (B1 and B2) immunoglobulin binding domains of Protein G.

Keywords

peptide structure; B3 domain of protein G; NMR; CD

INTRODUCTION

The mechanism by which proteins fold into their native conformations is one of the main unsolved problems of molecular biology. From the seminal work of Anfinsen and co-workers in the 1960's¹, it is known that the amino acid sequence of a polypeptide chain in the appropriate solvent environment fully determines its folding into its native conformation. Most small proteins can fold into a unique native conformation in less than 1s, and a few in even less² than 1 μ s. Misfolding can give rise to lethal diseases in humans or other animals^{3–5}.

Nowadays, due to the rapid development of new techniques such as protein engineering⁶ and kinetic analysis of folding, knowledge about protein folding has increased considerably. On the other hand, primarily due to limitations of these new techniques, knowledge about the earliest events of folding, which are the most important of the whole process, is incomplete⁷. It is very important to establish whether short protein fragments with a defined structure in the protein are able to adopt the same native structure when isolated. This will be possible only when such “folding intermediates” are detected and characterized. Thus, the only way to obtain insight into this process is to study the conformations of protein

fragments^{8–10}. Short linear peptides (<30 residues), in general, do not show marked conformational preferences in aqueous solution and, thus, until now, conformational studies were carried out only for peptides of special interest. However, in relation to the protein folding problem¹¹, it is very important to know if short protein fragments with a defined structure in the protein are able to adopt the same native structure when no tertiary interactions are yet present.

The B3 domain of protein G (PDB ID code 1IGD) from *Streptococcus sp.* (strain G148) (Figure 1) can serve as a model protein for studying the folding process of its fragments¹². 1IGD is a 61 residue protein, and its structure consists of two antiparallel-packed β -hairpins and an α -helix in the middle of the sequence packed to the β -sheet. The folding of the B1 and B3 domains of protein G has been studied extensively^{13–20} because they are stable globular folding units with no disulfide cross-links, with physical properties that offer extraordinary flexibility for evaluating the energetics of the folding reaction. These proteins are monomeric and very soluble in both folded and unfolded forms. Despite their small size and absence of disulfide bonds, the thermodynamics of the folding reactions is similar to that of larger proteins²¹. Kinetic analysis shows that no equilibrium intermediates are observed, and the folding process can be described by a two-state model^{13·15}.

Domains B1 and B3 of the immunoglobulin binding domain of protein G possess an identical three-dimensional fold and amino acid fragments which form an α -helix in both proteins. The α -helix differs in only two positions: Glu29 and Ala34 in the B3 domain are Ala and Val, respectively, in the B1 domain [the PDB codes of the three-dimensional structures are 1IGD and 2GB1, respectively]. The α -helical fragment is 16 residue long in both proteins. Blanco and Serrano²² reported a conformational study of the 20-residues long peptide that corresponds to the α -helical fragment of the B1 domain. This 20-residue long peptide is composed of the 16-residue α -helical fragment capped at the N and the C termini by two dipeptides whose sequence corresponds to the loop regions in the native structure of the B1 domain. This peptide was investigated extensively using CD and NMR spectroscopy both in aqueous solution and in a water/trifluoroethanol (7:3) mixture at 278 K. Blanco and Serrano concluded that the investigated peptide does not possess stable structure in aqueous solution, but forms an α -helix, especially at its N-terminus, in the water/trifluoroethanol (7:3) mixture. However, the chemical shifts of the H_N and H_α protons of the investigated peptide do not correspond to a completely random or very dynamic conformation, which suggests that this peptide possesses some conformational preferences but does not form a helical structure.

In our present work, we have investigated the structure and conformational dynamics of the 16-residue fragment from residue 28 to 43, hereafter referred to as IG(28–43), corresponding exactly to the α -helical fragment of the B3 domain of the immunoglobulin binding domain of protein G.

In this study, our primary interest is to investigate the conformational properties of a given fragment of a protein, and eventually assess the implication of these conformational properties for the mechanism of folding of the whole protein. In such studies, proper selection of the fragment to be investigated is very important. The use of short peptides always leads to the question as to whether the selected fragment is the optimal one to take account of all necessary local interactions which are responsible for the specific conformational properties. The literature does not provide any systematic studies that could serve as a guide as to how to select protein structure fragments for conformational studies. In most similar studies, the peptide length was based on two criteria: a) the selected sequence in the three-dimensional structure of the whole protein should possess a well defined secondary structure; b) the amino acid residues which define the ends of the selected

sequence should maintain non-covalent interactions within the fragment rather than with a different part of the protein or with the solvent^{22,23}. For 1IGD, the α -helical region extends from residue 28 to 43. The Asp27 residue, which we omitted from our selected sequence, does not exist in the helical conformation ($\phi = -167.7^\circ$ and $\psi = 177.6^\circ$), and is almost completely exposed to the solvent environment. The other residue omitted from the selected sequence is Val44, which does not exist in the helical conformation ($\phi = -126.5^\circ$ and $\psi = -179.6^\circ$), and its side chain forms a strong hydrophobic contact with residues Leu17 and Val59, which are outside of our selected α -helical region. Thus, for our study, we selected the fragment from residue 28 to residue 43. Initially, we planned to use a peptide, with both N and C termini blocked, to fully correspond to the protein fragment. However, such a peptide is not soluble enough for NMR measurements. Blanco and Serrano already observed this solubility problem, and used a peptide with free N-terminal amino and C-terminal carboxyl groups²². Our peptide with a free N-terminal amino group and a blocked C-terminal group is sufficiently soluble, and we decided to use it in our measurements. We are aware that, generally a free N-terminal amino group leads to destabilization of helical conformations mainly because of its unfavorable interaction with the helix dipole moment^{24,25}. However, as we reviewed the literature describing peptides which form a substantial percentage of helical structure in solution, most of such peptides have a free N-terminal amino group (for a review, see reference 24).

This peptide was examined by CD spectroscopy at different pH's, temperatures and trifluoroethanol concentrations. We also determined its structure by NMR spectroscopy in water solution at three different temperatures (283, 305, and 313 K). Most NMR studies of peptides that are protein fragments are usually carried out at very low temperatures (below 283 K) to reduce conformational dynamics and stabilize the structure²⁶. When using short peptides as models of early stages of protein folding, conformational studies should be carried out at temperatures, which are as close as possible to the folding temperature of the whole protein under investigation, or at least in the range of temperatures in which folding of a given protein occurs (many proteins become denatured at low temperatures). It is usually very difficult or impossible to obtain interpretable NMR spectra at temperatures above 320 K because of fast exchange of all amide protons by deuterium from the solvent²⁷. The folding temperature of the B3 domain of the immunoglobulin binding domain of protein G is 355 K²⁸. Taking this temperature limitation into account, we could not obtain NMR spectra close to the folding temperature of the whole protein; on the other hand, most folding/refolding experiments for proteins, in general, are performed at or around "room temperature", i.e., in the range of 290–310 K²⁹. Obtaining NMR spectra of peptides in the temperature range of 290–310 K enables us to compare results of such experiments directly with data obtained for the whole protein.

RESULTS

CD measurements

The CD spectra of the B3 domain peptide IG(28–43) of protein G were recorded under different conditions: (a) a buffer solution with pH values from 3 to 9 at room temperature (Figure 2a), H₂O, 10%, 50% and 90% TFE/H₂O at room temperature (Figure 2b), and H₂O at three different temperatures 283, 305 and 313 K (Figure 2c).

A regular α -helix conformation is characterized by a positive band around 190 nm and by two negative bands around 209 and 222 nm, respectively³⁰. The CD spectra of the IG(28–43) peptide obtained in phosphate buffer at different pH values look very similar. At each pH, only one negative band is observed at about 198 nm. We observed that the minimum at 198 nm became deeper, and increased with increasing pH up to pH 7. In spectra recorded at pH 7, we observed formation of another minimum around 202 nm. Spectra recorded at pH 9

do not possess a minimum around 198 nm and, in the region of 190–210 nm, the ellipticity decreased, almost linearly, with decreasing wavelength. These slight changes in CD spectra are reflected in the change of the random coil content, calculated based on the SP22X-CONTINLL de-convolution method³¹, as shown by the data in Table 1. These data suggest that the random coil content decreases with increasing pH from 3 to 7, which is associated with an increasing content of ordered structure (mainly β -sheet). Further increase of pH (above 7) leads to an increase of random-coil content. However, it should be noted that, for all investigated pH values, the random coil content remains very high and never drops below 21% (for pH 7). This peptide possesses seven ionizable groups, three amino groups (the N-terminal amino group and two lysine side-chain amino groups), three carboxylic groups (two from glutamic acid residues and one from aspartic acid), and one tyrosine. The data shown in Table 1 suggest that, if the net charge of the molecule is zero (all ionizable groups, except tyrosine are charged at pH \sim 7), the structure of the peptide is more ordered than when the net charge of the molecule is different from zero (at pH below and above 7), when the peptide becomes less structured.

The presence of trifluoroethanol (Figure 2b) results in an increase of the amount of ordered structures of the investigated peptide (see Table 1). When the amount of trifluoroethanol is 10%, the minimum that occurs at 198 nm in water is shifted to lower wavelengths, and the ellipticity increases. When the percentage of trifluoroethanol increases to 50% or 90%, formation of a positive band at 194 nm and two negative minima are observed around 209 nm and 222 nm. This suggests that the population of α -helical structure increases with the increase of trifluoroethanol concentration; however, according to the data shown in Table 1, the overall estimated content of α -helical structure does not exceed 20.4%. Blanco and Serrano observed a similar behavior for the B1 helical peptide²². It is interesting to note that the population of turn structures increases, which is associated with a decreasing population of β -structure with increasing TFE concentration. On the other hand, the population of random coil structures decreases with increasing concentration of TFE from 10% to 50%, but no large changes are observed with further increase of the TFE concentration.

Figure 2c and Table 1 show the data for the temperature dependence of the CD spectra. As can be seen from Figure 2c, with increasing temperature the minimum at 198 nm shifts to higher wavelengths and the ellipticity increases; also, a new minimum appears around 222 nm in the spectra recorded at 313 K. Visual comparison of the CD spectra recorded by using increasing concentrations of TFE and increasing temperature (Figure 2b and 2c) shows similar trends; however, the amplitude of the observed changes in the CD spectra recorded in H₂O/TFE mixtures are much larger than those observed in the temperature-dependent CD spectra. Thus, even if we are able to identify small changes (trends) visually in the CD spectra, the amplitudes of these changes are so small that the de-convolution procedure does not reflect those changes. By analyzing the data from Table 1, we can see that the de-convolution procedure shows that the α -helical content changes by less than 2% as the temperature increases..

NMR measurements

A more detailed structural analysis was carried out using NMR spectroscopy. 2D NMR spectra of IG(28–43) were recorded in water at pH 5.7 at three different temperatures 283, 305 and 313 K to examine the influence of temperature on the structure. The chemical shifts of the proton resonances for the IG(28–43) peptide at 283, 305 and 313 K are in supplemental data, and the changes in the chemical shift of the amide protons at different temperatures are shown in Figure 3.

With increasing temperature, all H_N protons are shifted to lower ppm values (see Figure 3). The decrease in chemical shift values of the NH protons suggests that the electron density

increases with increasing temperature, which means that those protons are not involved in hydrogen bonds inside the molecule, or with water molecules³². As shown in Figure 3, a dramatic downshift of the H_N proton signal for the Lys9 residue is observed at 313 K. This dramatic downshift may possibly be associated with the presence of a direct interaction between this proton and the aromatic rings of Phe 8 or Tyr 1132. Blanco and Serrano observed similar downshift in their investigation of a peptide corresponding to the helical part of the B1 domain of the immunoglobulin binding protein G22.

In Figure 4, the ROE effects corresponding to interproton distances and the values of the $^3J_{NHH\alpha}$ coupling constants are presented for NMR measurements carried out at different temperatures.

In unfolded peptides, the $H_\alpha(i) - H_N(i)$ connectivities are not observed or they are much weaker than the sequential $H_\alpha(i) - H_N(i+1)$ connectivities³³, despite the fact that the maximum value of the $H_\alpha(i) - H_N(i)$ distance is 2.8 Å for a trans peptide bond³³. For the IG(28–43) peptide at all temperatures, no $H_\alpha(i) - H_N(i)$ connectivities are observed; only medium-strong $H_\alpha(i) - H_N(i+1)$ ROE connectivities are present, which suggests, that the peptide is unfolded at each of these temperatures.

Another indication that the peptide is unfolded or very dynamic is the absence of $H_N(i) - H_N(i+1)$ connectivities³⁴. In IG(28–43), no $H_N(i) - H_N(i+1)$ connectivity is observed in spectra recorded at 283 K and 305 K, but several such signals appeared in spectra recorded at 313 K. In spectra recorded at 305 K and 313 K, weak signals between side-chain protons in the ROE spectra are observed. As can be seen in Figure 4, at 305 K, weak $d_{Nsc}(i,i+3)$ interactions between Ala7-Gln10, Ala12-Asn15 and $d_{sc}(i,i+4)$ interactions between Lys6-Gln10 are observed, which suggest formation of a turn in the middle of the sequence. In spectra recorded at 313 K, weak $d_{Nsc}(i,i+3)$ signals can be seen between Thr3-Lys6, which suggests formation of turns of some kind or locally bent structure; this is supported by the appearance of weak or medium $H_N(i) - H_N(i+1)$ signals in the ROESY spectrum recorded at 313 K in the middle region of the sequence. No signals were observed between side-chain protons at 283 K. It should be noted, however, that the value of the $^3J_{NHH\alpha}$ coupling constant of the Phe8 residue at 283 K is very low (4.6 Hz). Such a low value suggests that this region of the peptide backbone may be bent and form a turn.

MD simulations

The structural data summarized in Figure 4 were used to carry out MD simulations of IG(28–43) with time-averaged restraints, in order to determine the structure of this peptide at various temperatures. In Figure 5–Figure 7, the most populated conformational families from molecular dynamics simulations using NMR structural data with time-averaged restraints, collected at 283, 305 and 313 K, respectively, are presented. All structures obtained using NMR restraints recorded at 283 K (Figure 5) exhibit one common structural element, which is a turn-like feature in the N-terminal part of the molecule. In three families, another turn-like structure around residues Phe8 and Lys9 can be observed. Both of these conformational features correspond to strong ROE peaks between residues 3 and 5 and low values (lower than 5.5 Hz) of the $^3J_{NHH\alpha}$ coupling constants for residues Thr3, Ala4 and Glu5 (see Figure 4) and to a very low $^3J_{NHH\alpha}$ coupling constant for the Phe8 residue. It is interesting to note that the most populated cluster (about 14.7% of the analyzed conformations) displays an α -helix-like feature (indicated by the helix cartoon, see Figure 5a) in the middle of the sequence.

The clusters of conformations obtained using NMR restraints from measurements at 305 K (Figure 6) are much more diffuse than those presented in Figure 5, which is consistent with the observation that the four most populated clusters represent only about 36% of all

analyzed conformations, whereas the four clusters of Figure 6 represent about 44% of all analyzed conformations. The main feature of the structures obtained at 305 K using NMR restraints is some sort of a turn in the middle of the sequence, the formation of which is related to the signals observed between residues 6 and 10, and between 7 and 10, in the ROE spectra at this temperature (see Figure 6). A similar turn-like feature at the same position of the sequence was observed at 283 K for conformers presented in Figure 5 but it was caused by a very low value of the $^3J_{\text{NH}\alpha}$ coupling constant for the Phe8 residue.

The four most populated clusters of conformations obtained using NMR restraints from spectra recorded at 313 K are shown in Figure 7. The most populated family of conformations (11.5% of all conformations analyzed) based on NMR data recorded at 313 K, is the almost-extended conformation (see Figure 7a); this probably reflects increased mobility of the peptide with increasing temperature. The second most populated family of conformations (Figure 7b) exhibits turn-like structure located on residues Lys6 and Ala7; the remaining parts of the structure remain extended. A turn-like structure located on residues Lys6 and Ala7 is also observed in the third and fourth families of conformations (see Figure 7c,d). This structural feature is associated with proton-proton contacts observed in the ROESY spectrum (see Figure 4c), especially the $d_{\text{Nsc}}(i,i+3)$ signal between residues Thr3-Lys6 and $\text{H}_\text{N}(i) - \text{H}_\text{N}(i+1)$ for residues from Thr4 to Ala7. In the third and fourth families of conformations (Figure 7c,d) another turn-like structure is observed around residues Lys9 – Tyr11. This structural feature is associated with weak $\text{H}_\text{N}(i) - \text{H}_\text{N}(i+1)$ and $\text{H}_\beta(i) - \text{H}_\text{N}(i+1)$ ROE signals observed between residues Lys9 and Gln10 (see Figure 4c). The structure in Figure 7d has a characteristic α -helix-like shape; however, the structure is stabilized only by side chain – side chain interactions, not by hydrogen bonds as expected for a regular α -helix.

It is interesting to note that, in the third family of conformations (Figure 7c), the aromatic ring of Phe8 and, in the fourth family of conformations (Figure 7d), the aromatic ring of Tyr11 is very close to the amide proton of residue Lys9 (the center of the aromatic ring is less than 5 Å from the amide proton); such a close interaction is not observed in any another family of conformations, which are presented in Figure 5–Figure 7. This observation can provide an explanation for the unusual downshift of the amide proton of Lys9 (Figure 3), observed only for spectra recorded at 313 K.

Based on MD trajectories, we calculated the populations of the α -helical states of all residues; a residue was considered to occupy an α -helical state if its ϕ and ψ values were in the G or A region of the Ramachandran map according to the notation of Zimmerman et al³⁵. The results are summarized in Table 2. It can be seen that, for residues 1 to 8 and residues 12 and 13, the helical content increases with increasing temperature. On the other hand, for residues 9 to 11, a sharp drop in helical content is observed with increasing temperature. The helical content calculated for residues 14 to 16 changes slightly with temperature change. The mean value of the helix content, calculated over all residues, increases very slightly with increasing temperature.

DISCUSSION

We have carried out an extensive spectroscopic study of the 16-residue peptide with the amino acid sequence of the middle α -helical fragment of the B3 immunoglobulin binding domain of protein G from *Streptococcus*. The CD data shown in Figure 2 suggest that increasing temperature leads to a slight increase of the α -helix content with increasing temperature; however, the results from de-convolution of the CD spectra do not support this observation. Our NMR study shows that the peptide does not form a stable three-dimensional structure in aqueous solution; however, it has a tendency to form turn-like

structures around residues 4 and 5 and/or 9 and 10. The tendency to turn formation depends on temperature. At the lower temperature (283 K) (see Figure 5), a turn-like structure is formed in both of these positions whereas, at 305 K (see Figure 6), the turn is observed only in the middle of the sequence (residues 9–10) and, at 313 K, a weak turn is formed in the N-terminal portion of the peptide (residues 4–5) (see Figure 7). At 313 K, one family of conformations is almost α -helical. The structure presented in Figure 7d, in the central part (from Glu 5 to Ala 12), has a characteristic α -helix-like shape; however, the structure is stabilized only by side chain – side chain interactions, not by hydrogen bonds as expected for a regular α -helix. The overall population of this helix-like structure observed at 313 K is very low (5.7%). Data presented in Figure 2, Figure 5–Figure 7 and Table 2 suggest a slight increase of the helix content with increasing temperature, associated with an increase of the population of amino acid residues in the helical conformation (see Table 2). However, the number of residues in the α -helical state in a given conformation is still too small to call this whole conformation an “ideal” α -helical structure³⁶.

From the point of view of the folding mechanism of the B3 immunoglobulin binding domain of protein G from *Streptococcus* protein, we can conclude that, for the investigated peptide, a stable α -helix does not form in the investigated range of temperatures, which supports the results of Blanco and Serrano²² obtained for a homologous peptide from the B1 immunoglobulin binding domain of protein G from *Streptococcus* (it should be noted, however, that Blanco and Serrano carried out their NMR measurements only at 283 K). Based on our results, the investigated part of the sequence, i.e., residues 28–43, is not likely to serve as a nucleation site for folding of the whole protein if we assume that the first step of folding involves formation of the secondary structure elements³⁷. On the other hand, if we assume the nucleation-condensation mechanism³⁷ of folding, our finding that the investigated peptide at 313 K can form an α -helix-like structure, which is stabilized by side chain-side chain interactions, supports the idea that this part of the sequence can serve as a nucleation center. We have observed that the terminal portions of the investigated peptide can form α -helix-like structures at higher temperatures (305 and 313 K) (see Figure 6–Figure 7 and Table 2) with the middle part remaining mostly unstructured or extended. This observation is in agreement with results presented by Kuszewski and coworkers¹⁴. They investigated the partially unfolded B1 domain of protein G at 308 K and found that the backbone amide protons of the α -helical part of the protein are well protected against fast hydrogen-deuterium exchange¹⁴. This observation can suggest formation of organized structure for this part of the sequence at a temperature around 308 K. Similarly, Kmieciak and Koliński in theoretical studies recently found that the unfolded/denaturated state of the α -helical part of the B1 domain of protein G has a shape and contact pattern similar to those observed in native state³⁸. Both studies support the idea that the α -helical propensity of the investigated peptide increases with temperature; however we cannot rule out the possibility that, for the whole protein, the part corresponding to native α -helix can be influenced by the remaining part of the protein even in the unfolded state. It is known that, for this family of proteins, peptides corresponding to the C-terminal β -hairpin (see Figure 1) can form structures similar to that observed in the structure of the whole protein, suggesting that they are nucleation centers for folding²². Based on this information, we plan to carry out conformational studies of peptides, which correspond to the middle α -helix and the C-terminal β -hairpin (34 residues in length) to determine whether the α -helix, which has marginal stability as a stand-alone element, is able to form a more regular α -helical shape in the presence of the C-terminal β -hairpin. Additionally we are carrying out conformational studies of different length fragments of the C-terminal β -hairpin of the protein G B3 domain separately. All of these studies are carried out under different temperature conditions to obtain as much information as possible about the folding and stability of this group of proteins and to show how the individual fragments influence each other's stabilities.

We should point out that so far all experimental studies of different fragments of different variants of protein G were performed at very low temperatures (below 290 K)^{18,22}, which is far below the folding temperatures of the whole proteins. Our study shows that the increase of temperature changes the conformational propensity of the investigated peptide and drives its shape closer to that which it assumes as a fragment of the native protein. However, we cannot rule out the possibility that increasing temperatures can unfold other peptides excised from the B domains of protein G, which possess well defined shape at low temperatures. To be able to determine the mechanism of folding of proteins based on conformational studies of their fragments, detailed conformational studies should be performed in as wide as possible range of temperatures.

MATERIALS AND METHODS

Peptide synthesis

The peptide: H-AETAEEKAFKQYANDNG-NH₂ was synthesized using standard solid-phase Fmoc-amino acid chemistry with a Milipore synthesizer. The resin, Tentagel R RAM (1g, capacity 0.19 mmol/g) was treated with piperidine (20%) in DMF, and all amino acids were coupled using the DIPCI/HOBt methodology. The coupling reaction time was 2 h. Piperidine (20%) in DMF was used to remove the Fmoc group at all steps. After deprotection of the last Fmoc *N*-terminal group, the resin was washed with methanol and dried *in vacuo*. Then the resin was treated with a TFA/water/phenol/triisopropylsilane (8.8/0.5/0.5/0.2) mixture (10 ml per one gram of resin) at room temperature for 2 h. The resin was separated from the mother liquid, the excess of solvent was evaporated to a volume of 2 ml, and the residue was precipitated from diethyl ether. The crude peptide was dissolved in a mixture of 11.5% CH₃CN in TEA/H₃PO₄ and was purified by reverse-phase HPLC using a Kromasil C₈ semi-preparative column (20 × 250 mm, 5 μm) with 16 ml/min elution and a 120 min isocratic mixture of 11.5% CH₃CN in TEA/H₃PO₄ to adjust the pH to approximately 7.0. The fractions containing pure peptide were lyophilized and the purity was confirmed by analytical HPLC and MALDI-TOF analysis (*M* = 1755.8 g/mol; the theoretical value of the molecular mass is 1755.86 g/mol).

Circular dichroism (CD) spectroscopy

CD spectra were recorded on a Jasco J-20 spectropolarimeter with 2 cm/min scan speed, and data were collected from 260 to 190 nm with a 1 mm path length quartz cell. The samples were dissolved and the CD was measured at room temperature in (i) phosphate buffer (pH 3–9) and (ii) water (pH 6.53) and water solution of CF₃CH₂OH [H₂O/CF₃CH₂OH was 9:1, 1:1 and 1:9 by vol.], and (iii) at three different temperatures (283, 305 and 313 K) in water. The final concentration of IG(28–43) was 0.01g/100 ml. The secondary structure content was calculated from CD spectra using the self-consistent method³¹.

¹H-NMR spectroscopy

NMR spectra of IG(28–43) were obtained on VARIAN 500 MHz and 600 MHz spectrometers. The following spectra were recorded: 1D H-NMR and 2D HNMR: DQF-COSY³⁹, TOCSY⁴⁰ (80 ms) (Figure 8), ROESY⁴¹ (200 and 300 ms) at 283, 305 and 313 K. The sample was dissolved in H₂O/²H₂O (9:1 by vol.) (pH 6.53) and the concentration of the samples was 4 mM. The spectra were processed using VARIAN 4.3 software (Varian Instruments, PaloAlto, CA, USA) and analyzed with the XEASY program⁴². The spectra were calibrated against the HDO signal taking into account the temperature drift of the reference signal given by the equation $\delta_{1H(T)} = 5.060 - 0.0122t + (2.11 \times 10^{-5})t^2$, where *t* is the temperature in °C⁴¹. Proton signals were assigned based on TOCSY spectra. The peptide sequence has been confirmed by ROESY spectra⁴². The chemical shifts are collected in Tables 1–3 of the Supplemental data. The coupling constants between NH and

H_{α} protons (${}^3J_{\text{HNH}\alpha}$) of IG(28–43) were obtained from the DQF-COSY and 1H spectra. The intensities of the ROE signals were estimated from the ROESY spectra. In Figure 8, the assigned TOCSY spectra and the amino acid spin systems are shown.

Three-dimensional structure calculations

The ROE inter-proton cross-peaks of IG(28–43) were derived from 2D H-NMR ROESY spectra, and vicinal coupling constants ${}^3J_{\text{HNH}\alpha}$ were obtained from 2D H-NMR DQF-COSY and temperature-dependent 1D H-NMR spectra. In the first step, the ROESY peak volumes were converted to upper distance bounds by using CALIBA44 of the DYANA package45. In the next step, torsion angles were generated using the HABAS algorithm46 of the DYANA package47, on the basis of the Bystrov-Karplus48 equation. The upper distance limits and torsional angles were used as restraints in molecular dynamics calculations.

Molecular dynamics simulations with the time-averaged methodology (TAV)49–51 were carried out with the AMBER force field52 using the AMBER 8.0 package51. The interproton distances were restrained with the force constant $k = 20 \text{ kcal}/(\text{mol} \times \text{\AA}^2)$, and the dihedral angles with $k = 2 \text{ kcal}/(\text{mol} \times \text{rad}^2)$, respectively. The dihedral angles ω were restrained with the center at 180° and $k = 10 \text{ kcal}/(\text{mol} \times \text{rad}^2)$. The improper dihedral angles centered at the C^α atoms (defining the chirality of the amino acid residues) were restrained with $k = 50 \text{ kcal}/(\text{mol} \times \text{rad}^2)$. Three sets of separate simulations, using the restraints from the NMR data collected at 283, 305 and 313 K, were run. All simulations were carried out in a TIP3P53 periodic water box at constant volume, with the particle-mesh Ewald procedure for long-range electrostatic interactions54–55. MD simulations with time-averaged restraints from these three different temperatures, were carried out with a time step of 2 fs56, and the total duration of the run was 2 ns. For every NMR restraint set, four independent TAV MD simulations were run at the following temperatures: N, 400, 500, 600 K (where N is the temperature of the NMR experiment, i.e., 283/305/313 K). By carrying out simulations at many temperatures, as good a sampling of conformational space as possible is ensured. From every trajectory, 500 conformations were collected. The structures from four trajectories, obtained from simulations performed using the same NMR restraint set, were combined together. After TAV MD simulations, we obtained three sets of 2000 conformation each (four runs, with 500 conformations from every run) corresponding to three NMR restraint sets recorded at different temperatures. All three sets of conformations were clustered separately, with the use of the MOLMOL program57. An RMS deviation cut-off of 5.0 Å was used in the clustering procedure. The clustering procedure provided 48, 24, 28 families of conformations, for simulations, which used NMR data, recorded at temperatures 283, 305 and 313 K, respectively. The four most populated families at each temperature were selected for presentation. The RMS deviation was calculated based on residues from 3 to 13. Terminal residues were excluded from comparison because of their high mobility, which caused a rapid increase in the number of conformational families during clustering.

Supplementary Material

Refer to Web version on PubMed Central for supplementary material.

Acknowledgments

This research was supported by NIH grant GM-24893 and by a Polish Ministry of Science and Higher Education grant DS 8372-4-01387-8.

REFERENCES

1. Anfinsen CB, Haber E, Sela M, White FH. *J. Proc Natl Acad Sci USA*. 1961; 47:1309–1314.
2. Baldwin, RL. Chapter 1. In: Buchner, J.; Kiefhaber, T., editors. *Protein Folding Handbook*. Part I. Weinheim: WILEY-VCH Verlag; 2005.
3. Masters CL, Beyreuther K. *Nature*. 1997; 388:228–229. [PubMed: 9230425]
4. Carrell RW, Gooptu B. *Curr Opin Struct Biol*. 1998; 8:799–809. [PubMed: 9914261]
5. Radford SE, Dobson CM. *Cell*. 1999; 97:291–298. [PubMed: 10319810]
6. Serrano L. *Curr Opin Struct Biol*. 1994; 4:107–111.
7. Kuwajima K, Semisotnov GV, Finkelstein AV, Sugai S, Ptitsyn OB. *FEBS Lett*. 1993; 334:265–268. [PubMed: 8243629]
8. Baldwin RL. *Trends Biochem Sci*. 1986; 11:6–9.
9. Wright PE, Dyson HJ, Lerner RA. *Biochemistry*. 1988; 27:7167–7175. [PubMed: 3061450]
10. Dyson HJ, Wright PE. *Curr Opin Struct Biol*. 1993; 3:60–65.
11. Creighton TE. *J Phys Chem*. 1985; 89:2452–2459.
12. Derrick JP, Wigley DB. *J Mol Biol*. 1994; 243:906–918. [PubMed: 7966308]
13. Alexander P, Orban J, Bryan P. 1992; 31:7243–7248.
14. Kuszewski J, Clore GM, Gronenborn AM. *Protein Sci*. 1994; 3:1945–1952. [PubMed: 7703841]
15. Orban J, Alexander P, Bryan P. *Biochemistry*. 1994; 33:5702–5710. [PubMed: 8180196]
16. Orban J, Alexander P, Bryan P, Khare D. *Biochemistry*. 1995; 34:15291–15300. [PubMed: 7578145]
17. Kobayashi N, Honda S, Yoshii H, Uedaira H, Munekata E. *FEBS Lett*. 1995; 366:99–103. [PubMed: 7789539]
18. Blanco FJ, Rivas G, Serrano L. *Nature Struc Biol*. 1994; 1:584–590.
19. Sheinerman FB, Brooks CL. *J Mol Biol*. 1998; 278:439–456. [PubMed: 9571063]
20. Seewald MJ, Pichumani K, Stowell C, Tibbals BV, Regan R, Stone MJ. *Protein Sci*. 2000; 9:1177–1193. [PubMed: 10892810]
21. Alexander P, Fahnestock S, Lee T, Orban J, Bryan P. *Biochemistry*. 1992; 31:3597–3603. [PubMed: 1567818]
22. Blanco FJ, Serrano L. *Eur J Biochem*. 1995; 230:634–649. [PubMed: 7607238]
23. Dyson HJ, Merutka G, Waltho JP, Lerner RA, Wright PE. *J Mol Biol*. 1992; 226:795–817. [PubMed: 1507227]
24. Muñoz V, Serrano L. *J Mol Biol*. 1995; 245:275–296. [PubMed: 7844817]
25. Petukhov M, Yumoto N, Murase S, Onomura R, Yoshikawa S. *Biochem*. 1996; 35:387–397. [PubMed: 8555208]
26. Doig, AJ.; Errington, N.; Iqbalsyah, TM. Chapter 9. In: Buchner, J.; Kiefhaber, T., editors. *Protein Folding Handbook*. Part I. Weinheim: WILEY-VCH Verlag; 2005.
27. Baxter NJ, Williamson MP. *J Biomol NMR*. 1997; 9:359–369. [PubMed: 9255942]
28. Montelione GT, Tashiro M. *Curr Opin Struct Biol*. 1995; 5:471–481. [PubMed: 8528763]
29. Eaton WA, Muñoz V, Hagen SJ, Jas GS, Lapidus LJ, Henry ER. *Annu Rev Biophys Biomol Struct*. 2000; 29:327–359. [PubMed: 10940252]
30. Brahm S, Brahm J. *J Mol Biol*. 1980; 138:149–178. [PubMed: 7411608]
31. Provencher SW, Glockner J. *Biochem*. 1981; 20:33–37. [PubMed: 7470476]
32. Merutka G, Dyson HJ, Wright PE. *J Biomol NMR*. 1995; 5:14–24. [PubMed: 7881270]
33. Dyson HJ, Rance M, Houghten RA, Lerner RA, Wright PE. *J Mol Biol*. 1988; 201:161–200. [PubMed: 2843644]
34. Wüthrich K, Billeter M, Braun W. *J Mol Biol*. 1984; 180:715–740. [PubMed: 6084719]
35. Zimmerman SS, Pottle MS, Nemethy G, Scheraga HA. *Macromolecules*. 1977; 10:1–8. [PubMed: 839855]
36. Andrews MJI, Tabor AB. *Tetrahedron*. 1999; 55:11711–11743.
37. Nölting B, Andert K. *Proteins*. 2000; 41:288–298. [PubMed: 11025541]

38. Kmiecik S, Koliński A. *Biophys J*. 2008; 94:726–736. [PubMed: 17890394]
39. Piantini U, Sørensen OW, Ernst RR. *J Am Chem Soc*. 1982; 104:6800–6801.
40. Bax A, Freeman R. *J Magn Reson*. 1985b; 65:355–360.
41. Bax A, Davis DG. *J Magn Reson*. 1985a; 63:207–213.
42. Bartles C, Xia T, Billeter M, Güntert P, Wüthrich K. *J Biomol NMR*. 1995; 6:1–10.
43. Gottlieb HE, Kotlyar V, Nudelman A. *J Org Chem*. 1997; 62:7512–7515. [PubMed: 11671879]
44. Güntert P, Brawn W, Wüthrich K. *J Mol Biol*. 1991; 217:517–530. [PubMed: 1847217]
45. Güntert P, Mumenthaler C, Wüthrich K. *J Mol Biol*. 1997; 273:283–298. [PubMed: 9367762]
46. Güntert P, Braun W, Billeter M, Wüthrich K. *J Am Chem Soc*. 1989; 111:3997–4004.
47. Güntert P, Wüthrich K. *J Biomol NMR*. 1991; 1:447–456. [PubMed: 1841711]
48. Bystrov VF. *Progr NMR Spectrosc*. 1976; 10:41–81.
49. Torda AE, Scheek RM, van Gunsteren WF. *Chem Phys Lett*. 1989; 157:289–294.
50. Pearlman DA, Kollman PA. *J Mol Biol*. 1991; 220:457–479. [PubMed: 1856868]
51. Case, DA.; Darden, TA.; Cheatham, TE., III; Simmerling, CL.; Wang, J.; Duke, RE.; Luo, R.; Merz, KM.; Pearlman, DA.; Crowley, M., et al. AMBER8. San Francisco: Univ. of California; 2004.
52. Weiner SJ, Kollman PA, Nguyen DT, Case DA. *J Comput Chem*. 1986; 7:230–252.
53. Mahoney MW, Jorgensen WL. *J Chem Phys*. 2000; 112:8910–8922.
54. Ewald PP. *Ann Phys*. 1921; 64:253–287.
55. Darden T, York D, Pedersen L. *J Chem Phys*. 1993; 98:10089–10092.
56. Ryckaert JP, Ciccotti G, Berendsen HJC. *J Comput Phys*. 1977; 23:327–341.
57. Koradi R, Billeter M, Wüthrich K. *J Mol Graphics*. 1996; 14:51–55.

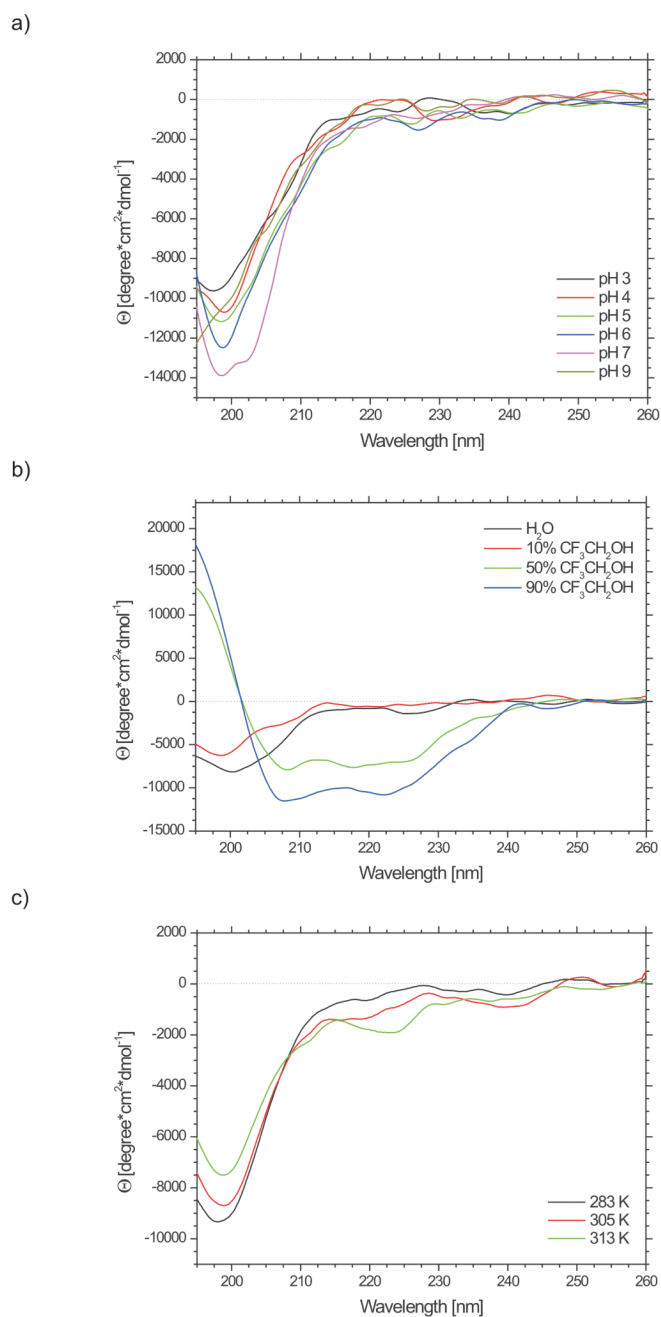


Figure 2. CD spectra of IG(28–43) in (a) phosphate buffer solutions, (b) water and water solutions of trifluoroethanol and (c) water at three different temperatures (283, 305 and 313 K).

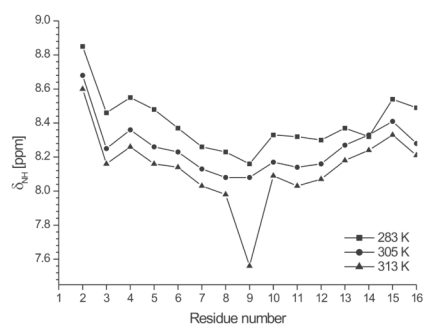


Figure 3. Chemical shifts of amide protons of each amino acid residue of IG(28–43) at pH=6.53 at three different temperatures (283, 305 and 313 K).

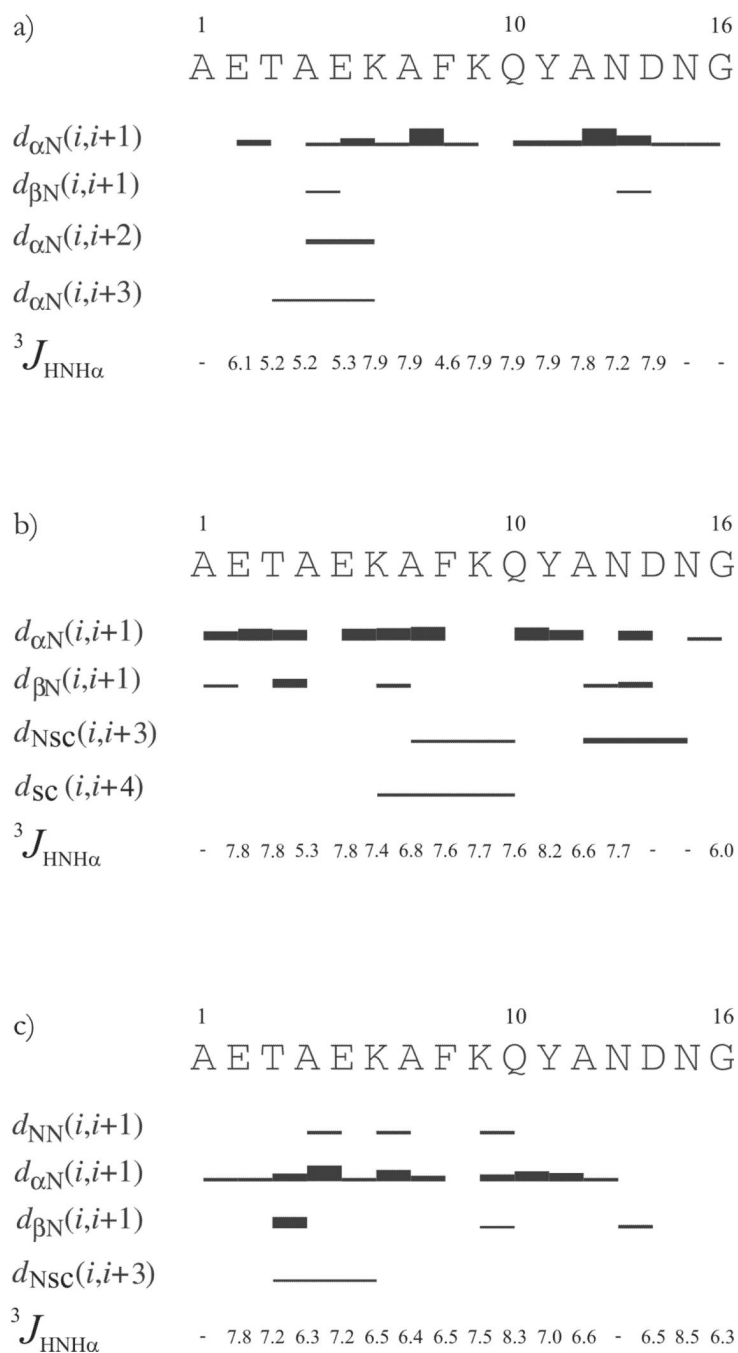


Figure 4. ROE effects corresponding to the interproton distances and the $^3J_{\text{NHH}\alpha}$ coupling constants of IG(28–43) measured in H₂O at (a) 238 K, (b) 305 K and (c) 313 K. The thickness of the bars reflects the strength of the ROE correlation as strong, medium or weak.

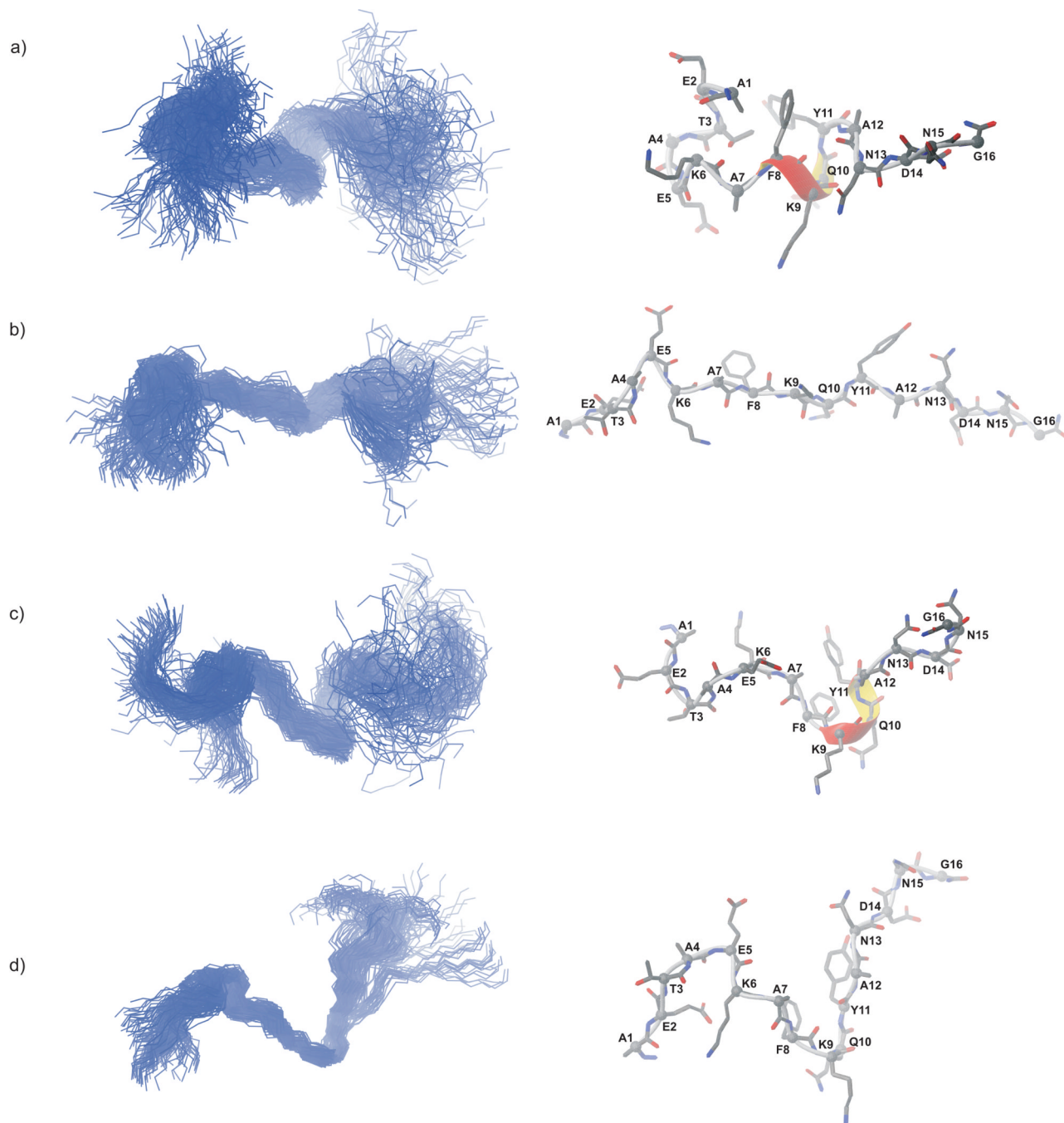


Figure 5.

Four most populated families of conformations of IG(28–43) obtained by using time-averaged MD methodology and data from NMR measurements at 283 K. Left column shows all conformations from a family (only backbones are shown for clarity), right column shows the lowest energy conformation from the corresponding family (all heavy atoms are shown). 2000 conformations were subjected to a cluster analysis, leading to the following relative population numbers and percentages of each clustered family: a) 294 (14.7 %), b) 204 (10.2 %), c) 194 (9.7 %), d) 188 (9.4 %).

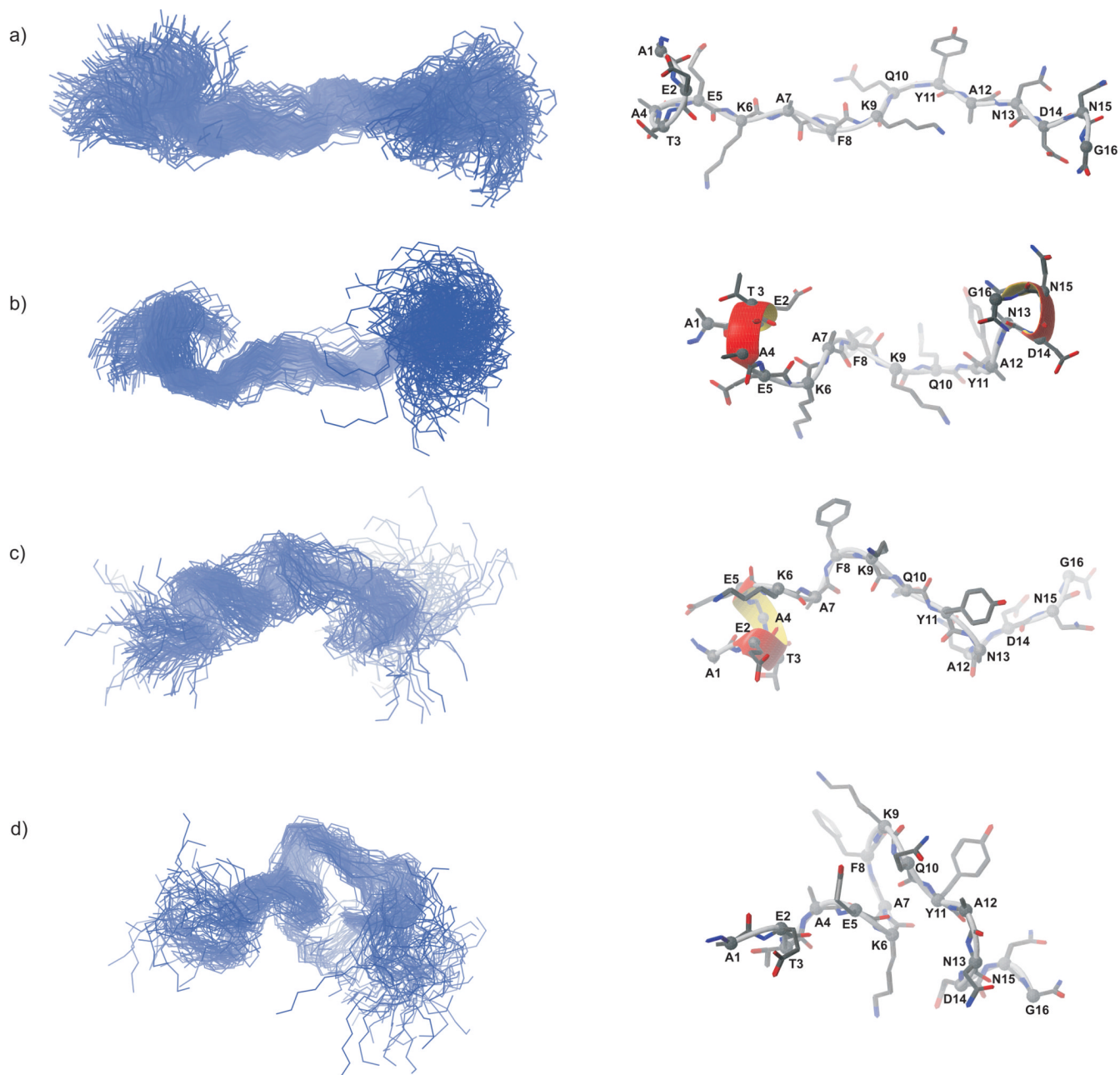


Figure 6. Same as Figure 5, but for 305 K, with the following results: a) 317 (15.8%), b) 185 (9.3%), c) 111 (5.6%), d) 108 (5.4 %).

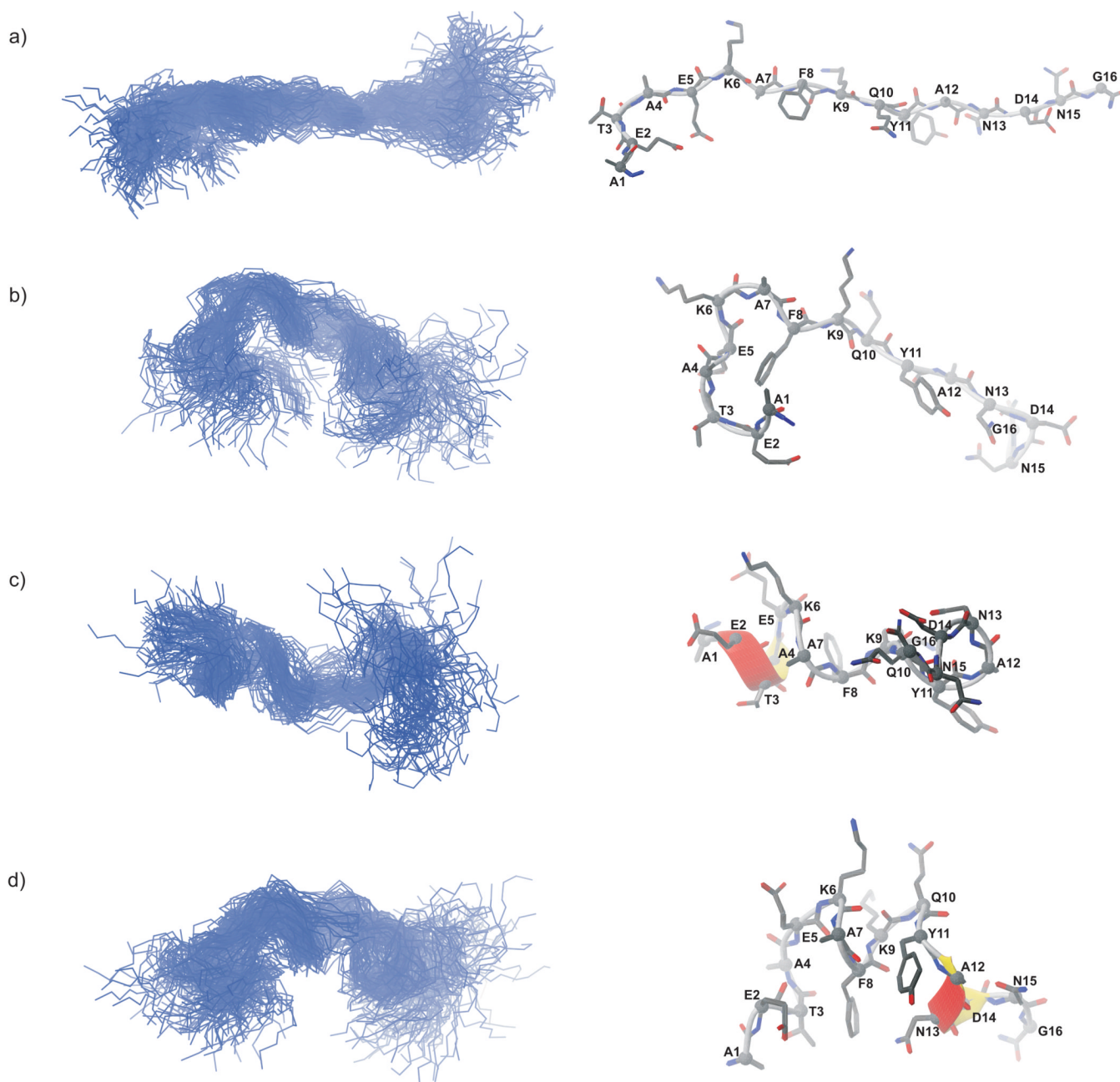


Figure 7.
 Same as Figure 5, but for 313 K, with the following results: a) 225 (11.5%), b) 137 (8.5%),
 c) 134 (6.9%), d) 113 (5.7 %).

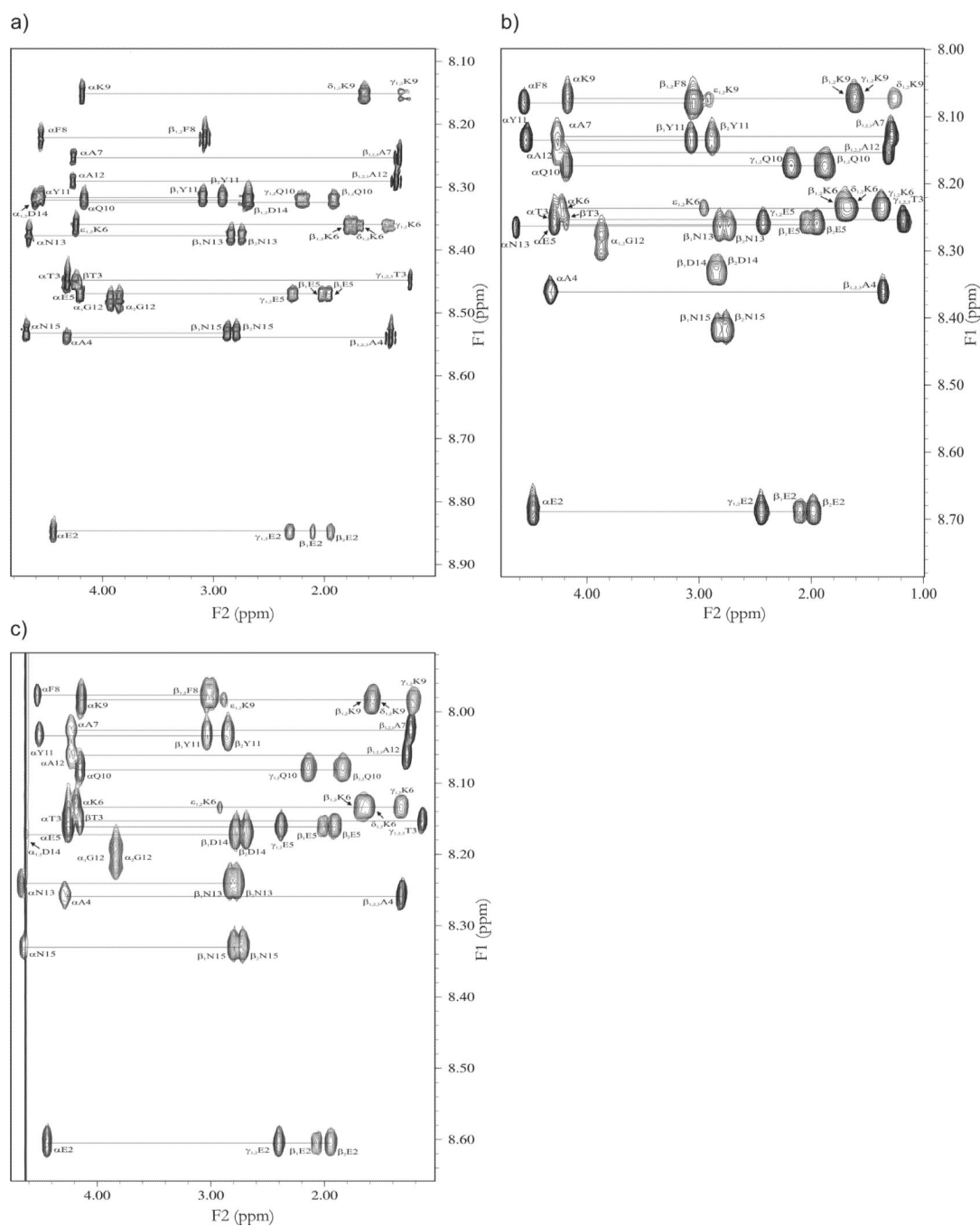


Figure 8. Amino acid spin systems in TOCSY spectra ($t_m = 80$ ms, diagnostic region) for IG(28–43) in H₂O at (a) 283 K, (b) 305 K and (c) 313 K.

TABLE 1

Percentage of secondary structure elements of IG(28–43) under different conditions obtained from CD spectra^a.

IG(28–43)	α -helix	β -sheet	turn	random coil	pp2
pH = 3	0.8	37.7	13.4	33.3	9.3
pH = 4	5.7	36.8	12.1	35.1	10.3
pH = 5	6.4	39.5	1.5	31.4	7.7
pH = 6	6.7	45.9	12.8	28	6.6
pH = 7	9.8	51.7	12.3	21.1	5.1
pH = 9	6.9	38.3	14	31.8	9
<hr/>					
10% TFE	4.8	32.4	13	38.7	11.1
50% TFE	8	28.3	23.8	30.8	9.1
90% TFE	20.4	19.6	26	31.7	2.3
<hr/>					
283 K	6.8	41.9	11.6	31	8.7
305 K	6.7	42	12.2	30.9	8.1
313 K	5.4	37.1	14	34.5	9.1

^aThe SP22X-CONTINLL method from Reference 28 was used to de-convolute the CD spectra.

TABLE 2

Percentage of helical conformation calculated for all residues using structures from TAV MD simulations performed with NMR restraints at three temperatures: 283, 305, 313 K. The first residue of the investigated peptide possesses the free N-terminal group which precludes a calculation of the ϕ angle for this residue.

	Residue number															
	2	3	4	5	6	7	8	9	10	11	12	13	14	15	16	mean
283 K	48.4	22.1	45	45.4	18.9	0	29	61.6	67.7	57.9	0	8.9	52.3	51.2	17.6	35.1
305 K	59.4	60.5	52.9	46.3	43.3	29.7	33.8	15.8	43.8	25.1	18	49.2	51	49.4	19.8	39.9
313 K	59.9	64.2	54.4	54.6	61.2	31.5	33.8	14.9	30.2	25.1	18	46	48.7	48.5	18.9	40.7